Journal of Trends in Computer Science and Smart Technology (ISSN: 2582-4104)
www.irojournals.com/tcsst/

Enhancing Insecticide Classification Accuracy with Modified ChemNet Architecture

Jubaira Mammoo[1], Malin Bruntha P.[2]

[1, 2]Department of Electronics and Communication Engineering, Karunya Institute of Technology and Sciences, Karunya Nagar, Coimbatore, Tamil Nadu, India.

Email: [1]jubaira2024@gmail.com, [2]malin.bruntha@gmail.com

Abstract

Proper detection of insecticides is also vital since it is the determinant of agricultural safety, efficiency, environmental protection and environmental compliance. In this paper, a modified ChemNet architecture is introduced, which is modified to the classification of insecticide in fruits. Compared to the traditional ChemNet, which leaves out chemical priors and residual learning, the proposed model has certain improvements: Squeeze-and-Excitation (SE) blocks for adaptive channel recalibration, residual blocks coupled with SE units to improve feature extraction, Self-Attention mechanism to learn long-range dependencies, and the swish activation function to support gradient flow and non-linear representation. Also, the network applies progressive dropout, early stopping, and class-weighted loss to address overfitting and unbalanced samples. The validation and training of the proposed model were trained using the Kaggle Banana Insecticide Dataset comprising a total of 6,103 images. The data is grouped into six distinct categories: monohigh (high level of banana treated with mono-type insecticide), monolow (low level of mono-type insecticide), novahigh (high level of nova-type insecticide), novalow (low level of nova-type insecticide), natural (banana samples that were never treated) and rotten (samples of banana that were biologically spoiled). This composition ensures that the dataset encompasses a wide range of levels of insecticide contamination and natural spoilage, enabling a strong foundation for training and evaluation. This will ensure the quality of the model in the classification of the data. The experimental findings show that the modified ChemNet achieves an overall classification accuracy of 81.02% and demonstrates good generalization across the chemically heterogeneous classes. These outcomes indicate the effectiveness of the proposed modifications to transform ChemNet for image-based insecticide detection in agricultural images and suggest its potential application as a tool for food safety monitoring that can be expanded.

Keywords: Insecticide, Vegetables and Fruits, Chemnet Model, Health Issues.

1. Introduction

The large-scale use of insecticides in contemporary farming has promoted the growth of crop yield to a considerable extent and has also provided protection to crops against predators, fungi, and weeds. However, this development comes at the price of the continued presence of insecticide residues in fruits and vegetables that form a significant segment of our

DOI: https://doi.org/10.36548/jtcsst.2025.3.012
Received: 11.07.2025, received in revised form: 13.08.2025, accepted: 30.08.2025, published: 16.09.2025

daily meals. These chemical residues may stay on the surface, or they may enter the inner tissues of the produce presenting a direct path of exposure to human consumers.

The residues can be the result of different phases of the agricultural process - direct application at the moment of cultivation, environmental contamination, and post-harvest treatment. Regulatory bodies have established maximum residue limits (MRLs) in food to promote food safety but there is scientific evidence that MRLs are not sufficient to ensure food safety when it comes to chronic, low-level doses of multiple pesticides over time.

Health risks linked to insecticide residues are both acute and chronic. Short-term exposure can lead to signs and symptoms that include skin irritation, gastrointestinal distress, and respiratory troubles. More concerning, long-term exposure, even in low concentrations, has been associated with cancers, neurological disorders (including Parkinson's and Alzheimer's), hormonal imbalances and reproductive complications. Susceptible populations-vulnerable groups, such as infants, children, pregnant women and farmworkers, at greater risk either physiologically or occupationally.

The correct and quick classification of insecticide residues on fruits and vegetables can be very difficult despite the rising awareness. Conventional methods of testing (e.g. chromatography, mass spectrometry) are accurate, but time-consuming, costly, and involve specialized equipment and expertise. These constraints have stimulated the development of non-invasive, image-based detection systems, especially those based on deep learning to identify visual signs of contamination by insecticides of various categories.

In this paper, we propose to use a deep learning framework to classify the level of insecticide contamination of fruit samples with a focus on developing a robust and scalable framework. To address this pressing concern, this paper formulates a powerful and scalable artificial intelligence model to categorize the level of insecticide contamination in fruit samples. The aim is to develop a precise, real-time, and accessible solution that complements regulatory systems to improve food safety and reduce health risks posed by chemical exposures.

Verger Philippe et al [1] showed that as many as 61% of the fruit and vegetables were above international Maximum Residue Limits (MRLs). The important finding is that 87% of the total 6,727 samples examined had MRL exceeding rates of more than 7% which contrasts with the 0.78% and 1.4% of samples exceeding limits in the USA and EU respectively. The presence of pesticide residues is a significant threat to public health, more so when most consumers in the area consume fruits and vegetables without washing or cooking them, subjecting them to further exposure to toxicants. Types of pesticides present include organophosphates and carbamates, which were the most common residues. The study also indicated that many of the samples contained numerous pesticides, which is a concern in terms of cumulative exposure effects on health. The study identified a lack of surveillance and control regarding pesticide application in the EMR. Improved policies, training of farmers on the safe use of pesticides and sensitization of people to the dangers of pesticide residues are necessary. To cope with health hazards, the paper proposes improvements in monitoring systems for pesticide residues, the implementation of stricter regulations on pesticide use, and the promotion of safer agricultural production methods among farmers. It is also proposed that public education campaigns be used to sensitize consumers to the proper handling of fruits and vegetables, thereby reducing exposure. In general, the present paper highlights a serious public health concern in the EMR involving agricultural operations and food safety, which must be addressed immediately since pesticide residue contamination poses a serious threat.

Renata Kazimierczak et al [2] evaluate the occurrence of pesticide residues in organic fruits and vegetables (apples, potatoes, carrots, and beetroots) marketed in Poland. Researchers analyzed 96 samples collected directly from organic producers in open markets using LC-MS/MS and GC-ECD/NPD systems to detect 375 pesticides. The findings indicated that 89 samples (92.7%) were pesticide residue-free. Nevertheless, 7 samples (7.3%) of carrots (5) and potatoes (2) contained detectable residues, one sample (1.0%) of which was above the maximum residue limit (MRL). Apple and beetroot samples contained no detectable residues. The research implies the necessity of intensifying monitoring of pesticides in organic produce, training farmers, and increasing public awareness of the dangers of unauthorized pesticide use to preserve the image of the organic industry.

The article by Mireya Povedano et al [3] discusses the levels of pesticide residues in organic vegetables and fruits (apples, potatoes, carrots, and beetroots) that are sold in Poland. Researchers processed 96 samples of food products taken directly from organic producers at open markets and tested them for 375 pesticides. During the analysis, pesticides were found to be free in 89 samples (92.7%). However, 7 (7.3%) out of 100 potato and carrot samples had pesticide residues and 1 (1.0%) of them was above the maximum residue limit (MRL). No pesticide residues were found in beetroot and apple samples. The authors propose enhancement of pesticide surveillance, training of farmers, and sensitization regarding the illegal use of pesticides to defend the brand image of the organic sector.

Narenderan et al. [13] provided a critical review of pesticide residues in fruits and vegetables analysis, as well as conventional techniques like GC and HPLC and new techniques involving nanotechnology and sensor development. Grimalt & Dehouck [15] reviewed analytical techniques used to identify pesticide residues in grapes and by-products, focusing on the fact that mass spectrometry combined with chromatography provides reliable results. Baca-Bocanegra et al. [18] investigated the possibility of using portable micro-NIR spectroscopy instruments to screen vineyards with respect to extractable polyphenols in red grape skins, and the results showed the potential of the method to evaluate quality without destroying the product. Lemos et al. [19] applied ATR-MIR spectroscopy with multivariate analysis to assist in the process of selecting clones of grapes from a variety called Tempranillo, successfully discriminating among grapes based on geographical origin and vintage year. Fernandez-Novales et al. [22] applied on-the-go VIS + SW-NIR spectroscopy to real-time measure grape composition in vineyards, aiding in making timely decisions regarding grape harvesting and processing. Costa et al. [23] constructed predictive models of quality and maturation stages of wine grapes based on VIS-NIR reflectance spectroscopy to optimize harvest times and enhance wine quality.

Jiang et al. [32] provide an innovative method for the non-destructive and rapid identification of pesticide residue in Brassica narinosa (black vegetable). The authors developed a multi-classifier combination algorithm, MCEWM (Multi-classifier Entropy Weight Method), that combines machine-learning classifiers SVM, Random Forest, and XGBoost with hyperspectral imaging. Alghawas et al. [34] establish the background and context of utilizing machine learning models to identify the presence of pesticide residues. The report discusses the widespread use of pesticides on farms, noting that much of this use has contributed to increased agricultural output. Concurrently, it highlights the dangers associated with pesticides, including environmental destruction and potential threats to consumers via food contamination. This paradox underlines the significance of adequate monitoring systems to keep food safe. The literature review examines traditional methods of identifying pesticide residues, which usually rely on chemical analysis. These methods are effective but labor-

intensive, expensive, and equipment-dependent techniques. This is why the task is one of the areas where machine learning techniques can introduce more effective solutions. The paper identifies previously conducted studies that have successfully applied machine learning techniques to various applications, such as food safety. It notes that machine learning algorithms are capable of handling large-scale data and identifying patterns that may not be detectable through more traditional means. This renders them suitable for the detection of pesticide residues in food samples. Another issue briefly addressed in the research is the necessity to compare different machine learning models to understand their applicability in specific applications. The research aims to contribute to the field of food safety by building on past studies and making contributions through the analysis of models such as K-Nearest Neighbors, Logistic Regression, Quadratic Discriminant Analysis, Naive Bayes, and Support Vector Machine. The survey reveals gaps in the current research, particularly in applying machine learning to detect pesticide residues. It emphasizes the need for further research and verification of these models to enhance their precision and effectiveness in real-life situations. To sum up, this survey clarifies the relevance of detecting pesticide residues with the help of new methods like machine learning while acknowledging the inefficiency of traditional techniques and the need for further studies in this direction. Figure 1 shows the proposed framework for the architecture of the modified Chemnet Model.

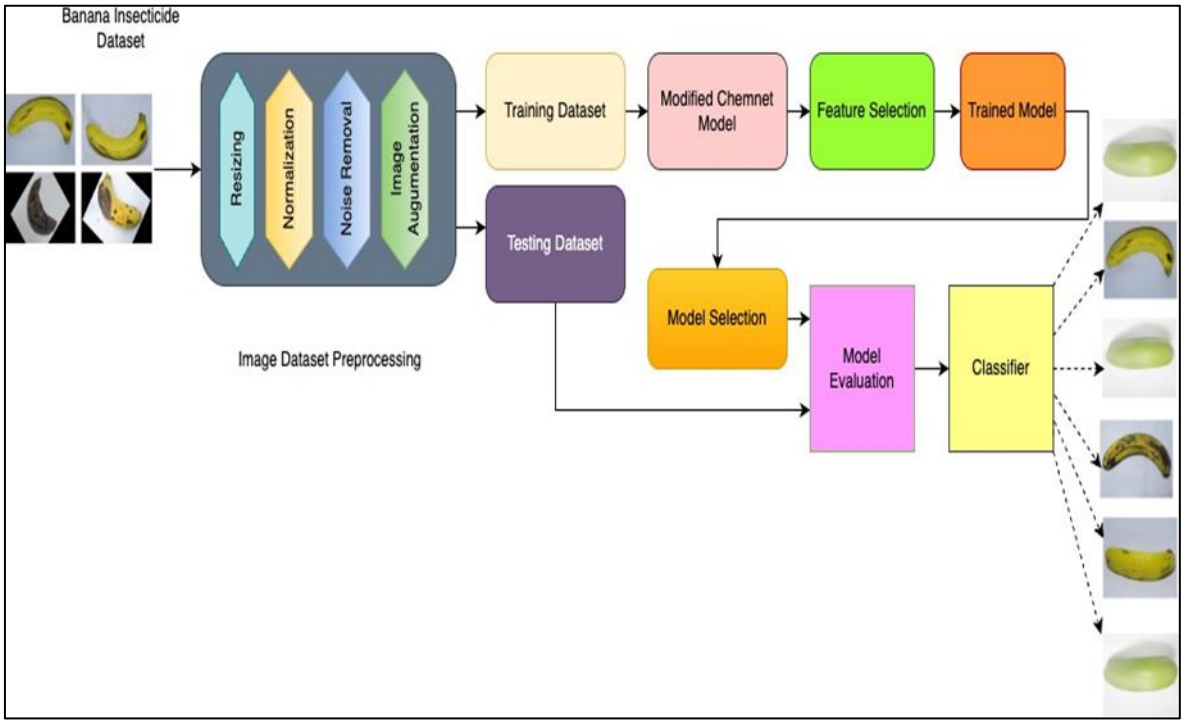

Figure 1. The Architecture of Modified Chemnet Model

2. Related Work

The study conducted by El-Sayed A et al [4] considers pesticide residues in vegetables, and fruits sold in farmer markets in Sharkia Governorate, Egypt, using LC-MS/MS and GC-MS/MS to identify the dietary risks involved. Forty of the pesticides were determined and the most prevalent were the insecticides. Cucumber and apple samples had the highest residues of pesticides. The mean residue levels were within 7-951 and 8-775 µg kg -1 of vegetable and fruit respectively. 35 (40.7%) out of 86 pesticide residues on vegetables and 35 (38.9%) out of

90 pesticide residues on fruits exceeded maximum residual limits (MRLs). Spinach, zucchini, kaki, and strawberry have acute or chronic risks at 0.1 and 0.2 kg day-1 consumption rates of lambda-cyhalothrin, fipronil, dimothoate, and omethoate, respectively. The results of the research emphasize the role of the constant control or monitoring of the pesticide residues on fruits and vegetables to maintain food safety and security.

Nabaasa Evarist et al [5] established a model to identify pesticide residues in common vegetables (tomatoes, cabbages, carrots and green pepper) sold in the city of Mbarara in Southwestern Uganda, based with image analysis. There were 1094 images of contaminated and uncontaminated vegetables taken on an InfiRay P2 pro Night Vision Go Mini Infrared Thermal camera. Noise removal, grayscale conversion, and image standardization were performed to do the Image Preprocessing. A python script was used to cluster the dataset with regards to chemical concentration rates. In Feature Extraction, a segmentation type of neural network that contained convolutional neural network, ReLu, max pooling, and fully connected layers was utilized in the extraction of features related to pesticide detection (mancozeb, dioxacarb, and methidathion). The images were classified according to pesticide concentration using Feature Classification by Convolutional neural networks transfer learning models (Inception V3, VGG16, VGG19, and ResNet50) and a scratch model. The research shows that the employment of artificial intelligence and infrared technology to check the presence of pesticide residues on vegetables is possible and will assist in solving problem of chemical contamination of food and food safety.

A model presented by Yating Hu et al. [6] was able to identify the presence of pesticide residues in the edible portions of tomatoes, cabbages, carrots, and green peppers. The researcher sought to establish a model to be used in detecting the presence of pesticide residues on common vegetables (tomatoes, cabbages, carrots, and green peppers) being sold in Mbarara City, Southwestern Uganda. Data collection involved taking 1,094 pictures of contaminated and non-contaminated vegetables with an InfiRay P2 Pro Night Vision Go Mini Infrared Thermal Camera. Noise elimination, conversion into grayscale, and standardization were used in image preprocessing. A Python script was run to cluster the data based on the rates of chemical concentration. A segmentation neural network consisting of convolutional, ReLU, max pooling, and fully connected layers was trained to extract features pertaining to the detection of pesticides (mancozeb, dioxacarb, and methidathion). The images were classified according to pesticide concentration using convolutional neural network transfer learning models (Inception V3, VGG16, VGG19, ResNet50) and a scratch model. The research shows that it is possible to identify pesticide residues on vegetables by means of artificial intelligence and infrared technology. A paper by Borza et al. [7] titled "Influence of Insecticides Used to Protect Stored Grain on the Technological Properties of Winter Wheat" was an attempt to test the effectiveness of varying doses of a pyrethroid insecticide against wheat weevil (Sitophilus granarius) and how it affected the quality of stored winter wheat. The test, which took three years on different grain silos, used 0.125 percent, 0.25 percent, 0.5 percent, and 1 percent dosing of the insecticides. Results showed that all the levels successfully destroyed the weevils in 8 hours, with the 1 percent dose recording the shortest time. Interestingly, the chemical composition and alveograph parameters analysis showed that the insecticide treatments did not negatively affect the technological quality of the wheat, allowing one to suppose that the insecticide may be used without negatively impacting grain quality. The ash content was very positively associated with the protein content.

Zhilong Kang, Yuchen Zhao et al. [8] experimented with the effectiveness of different concentrations of a liquid pyrethroid insecticide against Sitophilus granarius (wheat weevil)

and its influence on the technological properties of stored winter wheat. A three-year field experiment in grain warehouses tested the insecticide concentrations of 0.125%, 0.25%, 0.5%, and 1%. The results of the tests showed that all the concentrations were effective in killing the weevils within 8 hours, with the 1% dose being the fastest. It is interesting to note that the insecticide treatments did not reduce the quality of the winter wheat, as shown by chemical composition and alveograph parameters. Statistical analysis further showed that there was a significant positive correlation between protein and ash content. The study concludes that the tested formulation of pyrethroid can be used for the protection of stored grain without influencing the technological properties of wheat. Li et al. [9] applied near-infrared (NIR) spectroscopy and chemometric tools to perform a qualitative study on the determination of pesticides in purple cabbage. The research was very accurate, universal and suggestive of the use of NIR as a fast non-destructive test that could be used frequently.

Gowen et al. [10] studied hyperspectral imaging (HSI) as a new food quality and safety control method. HSI is a combination of imaging and spectroscopy to generate large volumes of spatial and spectroscopic data that are particularly suitable for measuring contaminants such as pesticides. Sun et al. [24] presented a quantitative method of detecting composite pesticide residues on lettuce leaves based on hyperspectral approaches. The method provided precise, non-destructive identification, and focused on the potential of HSI in monitoring pesticide residues. Jia et al. [25] suggested a hyperspectral imaging method to study pesticide residues on the surface of apples. This paper showed that HSI is viable and effective in sensing surface pesticide contamination. Moeder et al. [11] set up a procedure using membrane-assisted solvent extraction together with high-performance liquid chromatography-tandem mass spectrometry (HPLC-MS/MS) to measure 18 pesticides in red wine. The protocol provided good sample preparation and detection.

Simonetti et al. [14] compared gas chromatography (GC), liquid chromatography (LC), and capillary electrophoresis (CE) in determining Mancozeb, which is a commonly used pesticide. The paper discussed the pros and cons of each method and provided information about best practices in analytics. Zhang et al. [17] established and confirmed the technique of chiral separation and determination of diniconazole enantiomer residues in tea, apples, and grapes using supercritical fluid chromatography combined with quadrupole time-of-flight mass spectrometry (SFC-Q-TOF/MS). Bouagga et al. [12] analyzed 64 samples of Tunisian table grapes over 3 years, during which various pesticide residues were encountered in each sample, with an average of 11.6 residues. Of interest to consumers were the results of their exposure risks to pesticides.

Research Gaps Identified

Despite the high level of progress in pesticide detection with the help of analytical methods, machine learning, and deep learning revealed in the examined literature, several essential limitations still exist:

1. Excessive dependence on analytical methods developed in the laboratory. The current results provided using GC, HPLC, and LC-MS/MS have high accuracy but are not only time-consuming and expensive; they are also not applicable in real-time and large-scale applications. This limits their usage in the field.

2. Small dataset diversity and scope. The field has several methods that use small or region-specific data (e.g., a few hundred images or chemical samples). This is a major

limitation that makes the models weak and unrepresentative in terms of their application to various agricultural produce in different circumstances.

3. Binary detection focus. Previous studies focus mostly on binary classification (contaminated or uncontaminated). Multiclass classification to differentiate the level of exposure to pesticides is not emphasized much, which is important for monitoring food safety in detail.

4. Problems in sensitivity and specificity. Although machine learning algorithms and CNN-based models demonstrate promising results, they tend to fail in terms of sensitivity and specificity when detecting traces of pesticide residues or various types of pesticides in a single sample.

5. Explainability of deep learning models. More sophisticated deep neural networks, such as CNNs (Inception, ResNet, VGG16), have been implemented; however, they are less credible due to their explainability and lack of transparency and will be subject to regulatory restrictions.

6. Lack of scalable and real-time solutions. Few research papers have attempted to develop models for real-time automated pesticide detection. This underlines a discrepancy between research prototypes and deployable systems in food supply chains.

3. Proposed Work

To fill the gaps mentioned above, this paper presents a modified ChemNet architecture trained on an insecticide dataset (6,103 banana images in six exposure categories). The suggested method combines self-attention, SE blocks, and Swish activation, to enhance sensitivity, specificity, and interpretability. The model will be multiclass rather than binary as in previous methods because the subtle conditions of insecticide exposure require it. It aims to go beyond purely laboratory-based solutions and create a robust, scalable, efficient deep learning model to be used in the practical application of agricultural food safety.

Table 1 presents a comparative analysis of various methods for pesticide residue detection, highlighting the study, findings, methodologies, and recommendations from each research article. This underscores the need for a novel method that addresses these challenges and enhances the overall effectiveness of pesticide residue detection systems.

Table 1. Comparative Analysis of Various Methods for Pesticide Residue Detection

Author(s)	Objective	Methodology	Key Findings	Conclusion
Verger Philippe et al [1]	Review pesticide residue levels in fruits and vegetables	Literature review on MRL exceedances	Up to 61% of samples exceeded MRLs	Need for stricter control on pesticide residues
Renata Kazimierczak et al [2]	Evaluate pesticide residues in organic produce in Poland	96 samples analyzed using LC-MS/MS and GC-ECD/NPD	92.7% pesticide-free 7.3%	Strengthen monitoring and educate organic farmers

			contaminated (mainly carrots and potatoes)	
Mireya Granados-Po et al [3]	Similar to povedan (duplicate study) [2]	Same methodology as [2]	Same findings as [2]	Same conclusion as [2]
El-Sayed A. El-Sheikh et al [4]	Investigate pesticide residues in Egyptian fruits and vegetables	LC-MS/MS and GC-MS/MS on samples from markets	40 pesticides detected, many exceeded MRLs, health risks noted	Continuous monitoring emphasized for food safety
Nabaasa Evarist et al [5]	Detect pesticide residues via image analysis in Uganda	Infrared imaging + CNN models (Inception V3 best)	Inception V3 achieved 96.77% accuracy	AI shows potential in pesticide detection
Yating Hu et al [6]	(Duplicate of [5]) Detect pesticide residues via image analysis	Same as [5]	Same as [5]	Same as [5]
Borza, Gavrilaˇ et al [7]	Assess impact of insecticides on stored wheat quality	Tested different insecticide concentration against weevils	Effective elimination, no negative effect on wheat quality	Pyrethroid safe for grain storage
Zhilong Kang, Yuchen Zhao et al [8]	(Duplicate of [7]) Effectiveness of pyrethroid insecticide on wheat	Same as [7]	Same as [7]	Same as [7]

4. Methodology

Under this proposed method, the model will load images of fruits (bananas) to be analyzed. The raw images are then followed by a series of preprocessing steps to ensure that the data is of high quality and uniformity. These steps include resizing, normalization, and noise removal. Rotation, flipping, zooming, and shifting data augmentation methods were used so that the training set could be further extended and better models could be generalized. Figure 3 shows the general flow of the chemical detection process. The proposed deep learning models were trained after preprocessing and augmentation to categorize the fruits as pesticide-contaminated or pesticide-free. This approach uses the performance of our model against standard baselines to evaluate the feature extraction capacity. To make decisions, the classification module of the model offers the probability of each image belonging to the various classes, which is compared to a specified threshold value. Finally, the learned model is applied to make predictions on new data, generating actionable outcomes that represent the toxicity

status of each fruit. This setup is relevant for training and testing deep learning models in PyTorch. Classes: [’monohigh’, ’monolow’, ’natural’, ’novahigh’, ’novalow’, ’rotten’]. Using this structured pipeline, the deep learning method described in this paper would yield a highly accurate and reliable solution to the problem of pesticide contamination in fruits. The training, testing, validation, and development phases of the proposed modified Chemenet architecture are represented in Figure 2.

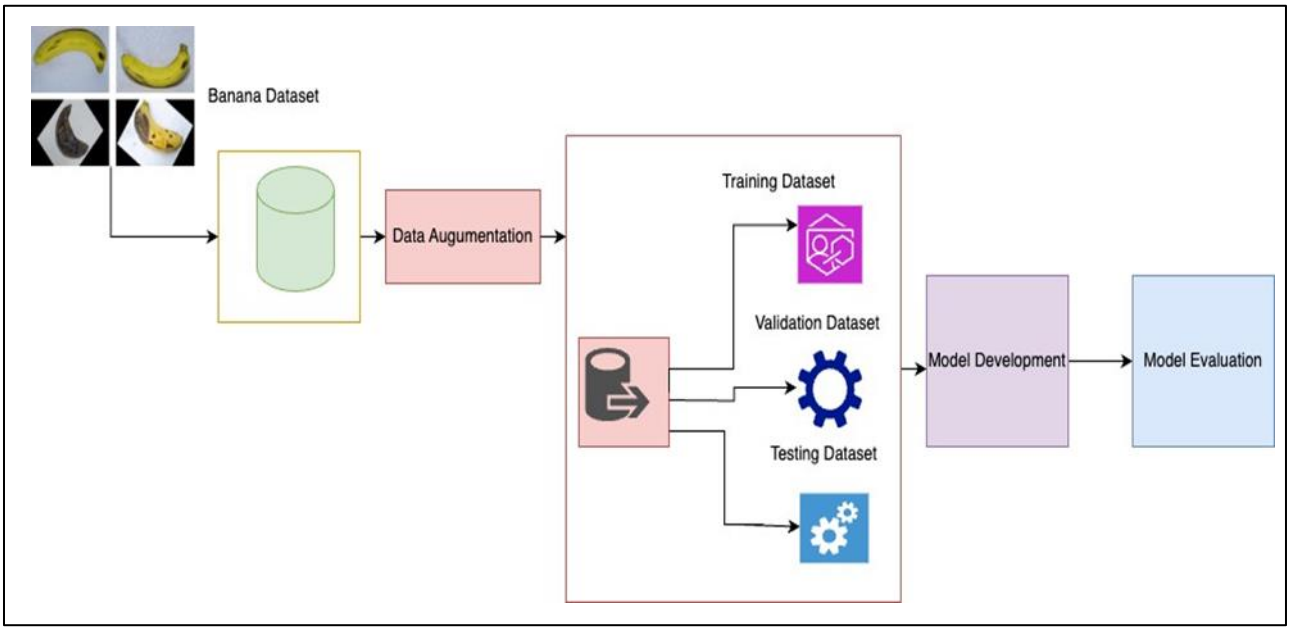

Figure 2. Testing, Validation and Development Phase of the Proposed Modified Chemenet Architecture

The architecture has an input layer that takes RGB images of 224x224x3 and normalizes them to ImageNet statistics. Low-level features of edges and color gradients are extracted by an initial convolutional layer with a 7x7 kernel, a stride of 2, batch normalization, and Swish activation. This is followed by a sequence of residual block layers, the first of which contains two 3x3 convolutional layers with batch normalization, a Swish activation function, and a Squeeze-and-Excitation (SE) block within a ResNet style, skip connection to provide channel wise feature recalibration, The second residual block layer increases filter depth (64→128) and down samples to capture more abstracted representations and address spatial resolution, while the third residual block further increases channel depth (128→256), with SE blocks and Swish activation to learn deeper semantic patterns. To supplement these local properties, a query key value self-attention mechanism and a parameterized parameter are added to the model, to establish long-range range spatial connections and connect the spread apart contamination areas. The result of hierarchical feature extraction is compressed into the spatial dimensions by global average pooling, and is further fed into fully connected layers with batch normalization, Swish activation, and dropout regularization, to make final predictions through a Softmax classifier across six classes (monohigh, monolow, novahigh, novalow, natural, and rotten). To further enhance generalization and stability in training, the model employs regularization methods like early stopping on validation loss, weighted cross entropy loss to address class imbalance, and as many data augmentation methods as possible like rotation, flipping, and normalization. Such an integrated architecture effectively combines residual learning, attention, and adaptive feature recalibration to generate robust and accurate insecticide residue classification.

4.1 Flow Diagram

Flow diagram of the proposed Modified ChemNet-based insecticide classification framework is shown below in Figure 3.

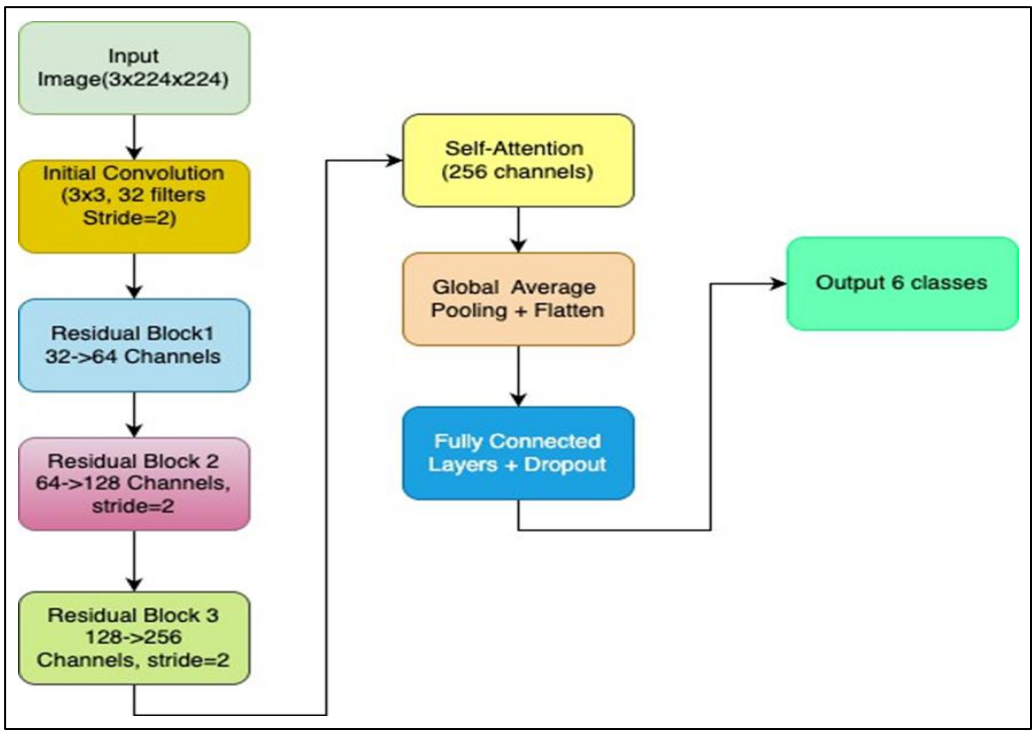

Figure 3. Flow Diagram

4.2 Dataset

The model is proposed to be trained, tested, and validated using different datasets from public repositories. The creation of the dataset has been done using the Kaggle banana insecticide datasets [31]. Table 2 illustrates how the datasets contribute to the formulation of the proposed framework. The data utilized in this research paper consists of banana images that are categorized according to different insecticide conditions. The Table 2 dataset distribution of insecticide image classification provides a summary of the dataset that was used in the training and testing of the insecticide model. The study utilized a total of 6,103 images, with 5,082 for training and 1,021 for testing. It is a typical machine learning setup in which most data is held out to train a model, but a small, separate set is used to test its capacity to work on previously unseen data. The data is a collection of photos with various insecticide states on fruits or vegetables and forms the foundation for training deep learning models to classify and identify the correctness of insecticide presence. This training set is large and balanced, which ensures good learning, and the testing set provides a good estimate of the generalization performance of the model. The categories present in the dataset are monohigh, monolow, natural, novahigh, novalow, and rotten; this allows training the models to distinguish small differences that relate to the application of insecticides and the resultant conditions. The sample images of the banana dataset are in Figure 4. The banana dataset classification is as follows.

1. **Monohigh:** Bananas treated with a high level of monotype insecticide. These often show minimal surface alterations due to chemical residue.

2. **Monolow:** Bananas treated with a low-level monotype insecticide. They have a more natural appearance but contain mild chemical effects.
3. **Natural:** Untreated bananas, where no insecticides or chemicals have been applied. These serve as the control sample for comparison purposes.
4. **Novahigh:** Bananas treated with a high dose of nova-type insecticide. The surface might develop discoloration or residue impacts from more intense chemical treatment.
5. **Novalow:** Bananas with a reduced nova-type insecticide dosage, showing little residue and largely maintaining a natural appearance.
6. **Rotten:** Bananas that have been biologically spoiled. These exhibit visible decay, discoloration, or texture loss, useful in distinguishing chemical versus natural spoilage.

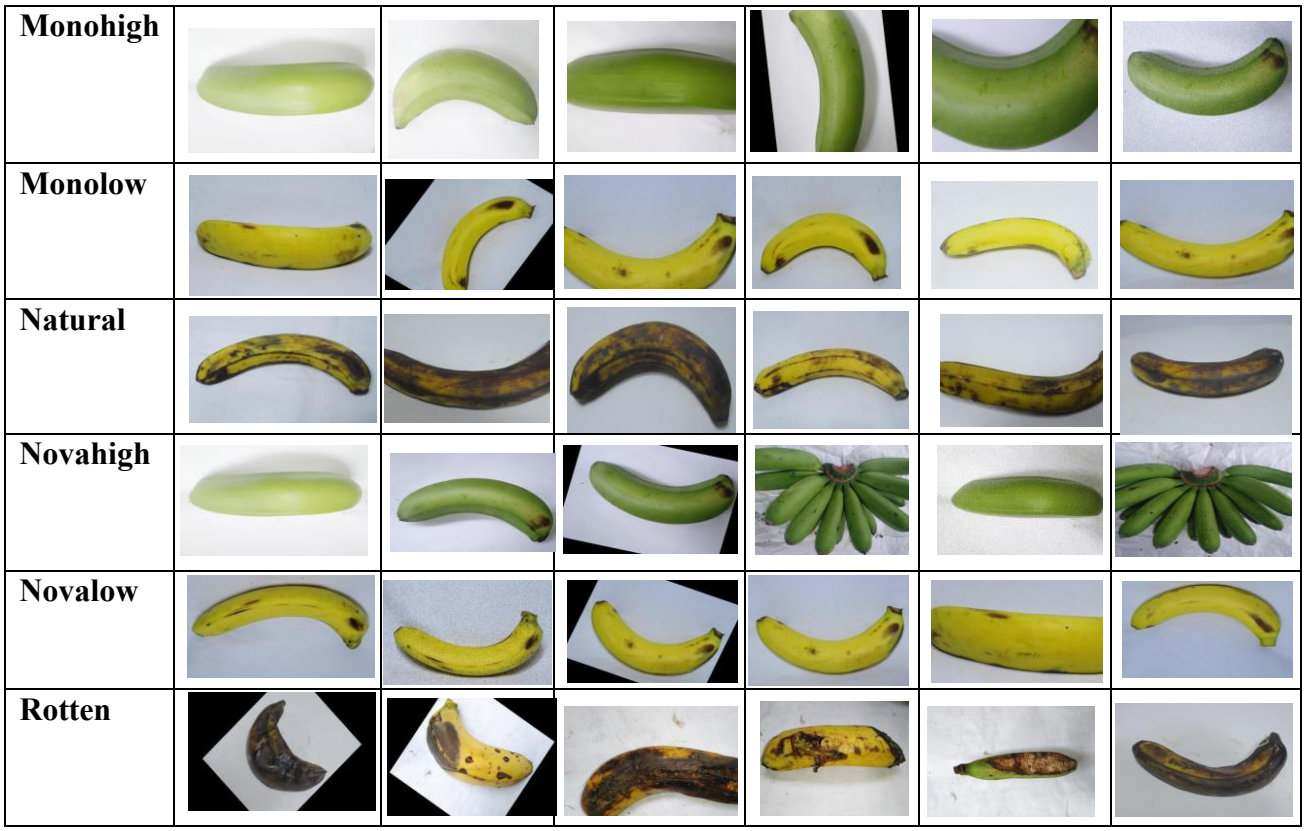

Figure 4. Six Sample Images from Each Class

Table 2. Dataset Distribution for Insecticide Image Classification

Data Condition	Training	Testing	Total
Insecticide Images	5082	1021	6103

4.3 Feature Extraction

Squeeze-and-Excitation (SE) block is formulated in feature extraction, an element in deep neural networks that behaves adaptively to recalibrate channel wise feature responses. It starts with an adaptive average pooling layer which decreases the spatial dimensions to 1x1, i.e. squeezes the spatial information into a single value per channel. These values are then down scaled by a factor of reduction, the ReLU activation is applied and then scaled back to the original dimension using a sigmoid activation to produce scaling factors between 0 and 1. During the forward pass, input data is first squeezed into a smaller shape after which it is run through these fully connected layers to generate scaling factors, and then stretched back to original input dimensions. Finally, these scaling factors multiply the original input and in effect they rescale the importance of each channel in the feature maps. The operation allows the model to channel selectively what to listen to and gives it better performance when used in tasks like image classification and object detection. The feature extraction process that is employed in this study to develop the proposed modified Chemnet architecture is presented below in Figure 5.

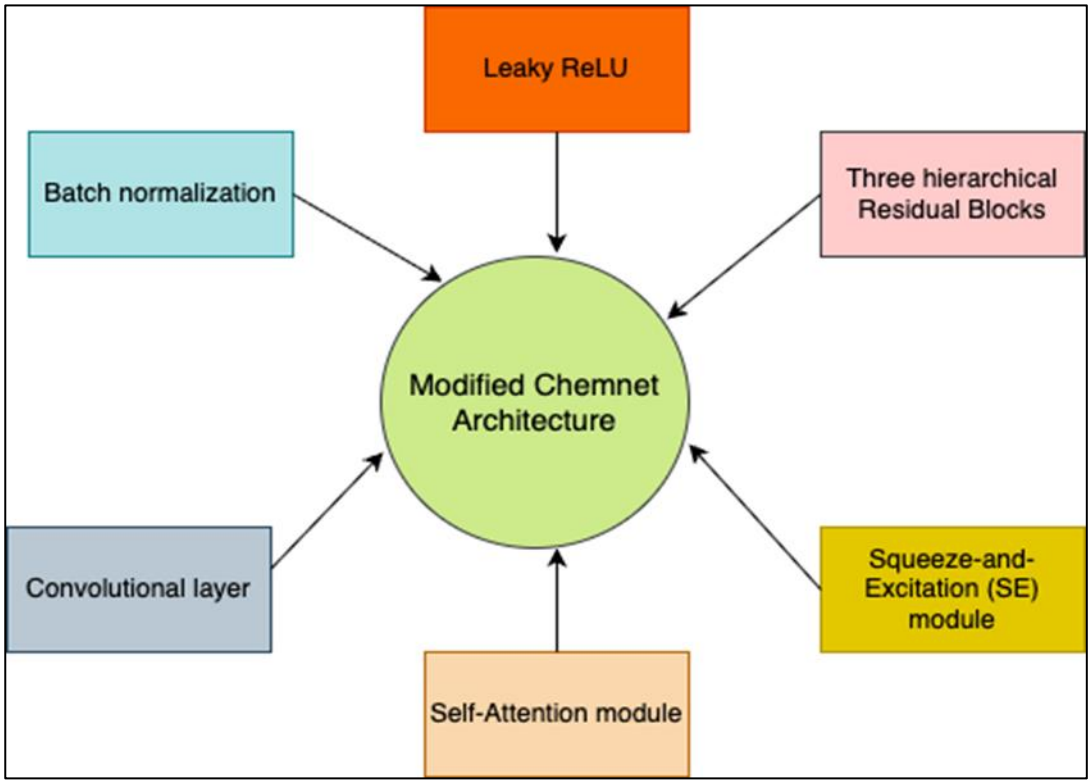

Figure 5. Feature Extraction Process Adopted in this Research for the Development of the Proposed Modified Chemnet Architecture

4.4 Classification

We have already applied the Residual Block in deep learning classification which is the building block of ResNet architectures. The Residual Block is designed to learn residual functions with respect to the layer inputs, which can be helpful in training deeper networks. It consists of two convolutional blocks (conv1 and conv2, each possessing batch normalization) and a Squeeze-and-Excitation (SE) block, which is used to dynamically weigh channel

importance. The first convolution (conv1) can down sample the spatial dimensions in terms of stride, while the second one (conv2) will retain them. The identity connection has optional downsampling when spatial dimensions need to be down sampled. The forward pass includes these layers and the SE block to which the input is fed and added to the identity connection (which might be downsampled). The result is then passed through a Leaky ReLU activation function so that the block can learn sophisticated representations without destroying the negative values. This structure does not suffer from the problem of vanishing gradients and enhances the model's capability to learn deep representations.

The Residual Block, which is a core building block in ResNet models, is applied to train deep neural networks where learning occurs in residual functions. This block starts with two convolutional layers (conv1 and conv2), each followed by a batch normalization block, and a Squeeze-and-Excitation (SE) block that allows for dynamically changing the relative importance of channels. Conv1 uses a given stride to reduce the spatial dimensions whereas conv2 keeps the spatial dimensions unchanged. The identity connection can be assigned a downsampling path (downsample), if spatial dimensions need to be downsized. These layers plus the SE block are used in a forward pass to process the input through the layers, and the identity connection (which may be downsampled). The output is then subjected to a Leaky ReLU activation function which introduces nonlinearity without removing negative values. The architecture helps reduce vanishing gradients and can also better learn powerful representations as it specializes in the differences between the layers rather than attempting to learn the entire input-output mapping.

SelfAttention: The SelfAttention class calculates self-attention on convolutional feature maps to enable the model to form long distance connections. It first applies 1x1 convolutions to generate query (Q), key (K) and value (V), with Q and K downsampled in dimension to save computation cost, while V maintains the same number of channels. The attention scores are obtained by taking the dot product of Q and K and normalizing them with a softmax. The V matrix is then weighted using the attention map generated, reinforcing important elements in space. The output is the combination of the initial input and attention weighted features multiplied by a learnable parameter (gamma) that is initialized to 0, allowing the network to gradually the impact of attention. This mechanism can help improve feature representation showcasing important areas with a residual connection to stable learning.

ChemNet architecture is a convolutional neural network, applied to analyze chemical images, and includes residual blocks and self-attention. It begins with a downsampling convolution (3x3, stride 2) which halves the spatial resolution but expands to 32 channels, followed by batch normalization and LeakyReLU activation. These residual block levels successively increment feature depth (64 - 128 - 256 channels) and opportunistically use stride=2 convolutions to reduce spatial dimensions. The self-attention module in the deepest layer enables the mapping of long-distance spatial relationships in the feature maps.

Classification utilizes adaptive average pooling to downsize spatial dimensions that follow the features into a multi-layer classifier that has batch normalization, leaky ReLU activations and progressive dropout (0.5→0.4) regularization. The design is a trade-off between hierarchical feature extraction (through residual blocks) and global context modeling (through attention), which is especially a good fit to the tasks of chemical structure recognition where both local pattern recognition and global compositional interpretation are needed. The core training infrastructure for ChemNet involves (1) instantiating the model with the output neurons corresponding to the number of classes in the dataset and mounting it to the targeted hardware (GPU/CPU), (2) configuring CrossEntropyLoss to work on multi-class classification

by estimating the difference between logits and true labels, and (3) initializing the Adam optimizer with the learning rate set to 0.001 to update the model weights via the gradient. The components are connected during training, and the model is fed the input data (forward pass), The loss measure is calculated as the degree of accuracy of the prediction, the gradients are calculated (backward pass), and Adam updates the parameters to reduce the loss. This configuration is especially useful in the analysis of chemical data, where adaptive learning rates (Adam strength) can help overcome different feature scales, and the implicit softmax loss function can be beneficial in tasks that involve categorical losses such as chemical classification tasks. To improve performance, one can add learning rate scheduling or class weighting later in the case of imbalanced chemical data.

The train model function performs an entire training iterates that repeatedly loops over a set of epochs, executing forward propagation, loss computation, backpropagation and parameter updates with the training data loader, and validating performance periodically. Each epoch begins by putting the model in train () mode (enabling dropout/batch normalization), looping through batches with a transfer of data to the compute device (GPU/CPU), computing predictions and loss, and then resetting any previous gradients (zero grad()) before error backpropagation and weight updating by optimizer.step(). The loss during training is cumulative and averaged over each epoch, and intermediate results are printed as it progresses. After every training step, the validate model function is invoked (presumably in evaluation mode and with gradients turned off) to evaluate the validation set. This framework allows for cyclical parameter optimization and helps avoid overfitting with regular validation by allowing batch wise processing of large chemical data, which can be processed efficiently using a small amount of memory. Figure 6. refers to the suggested approach for the classification of pesticides.

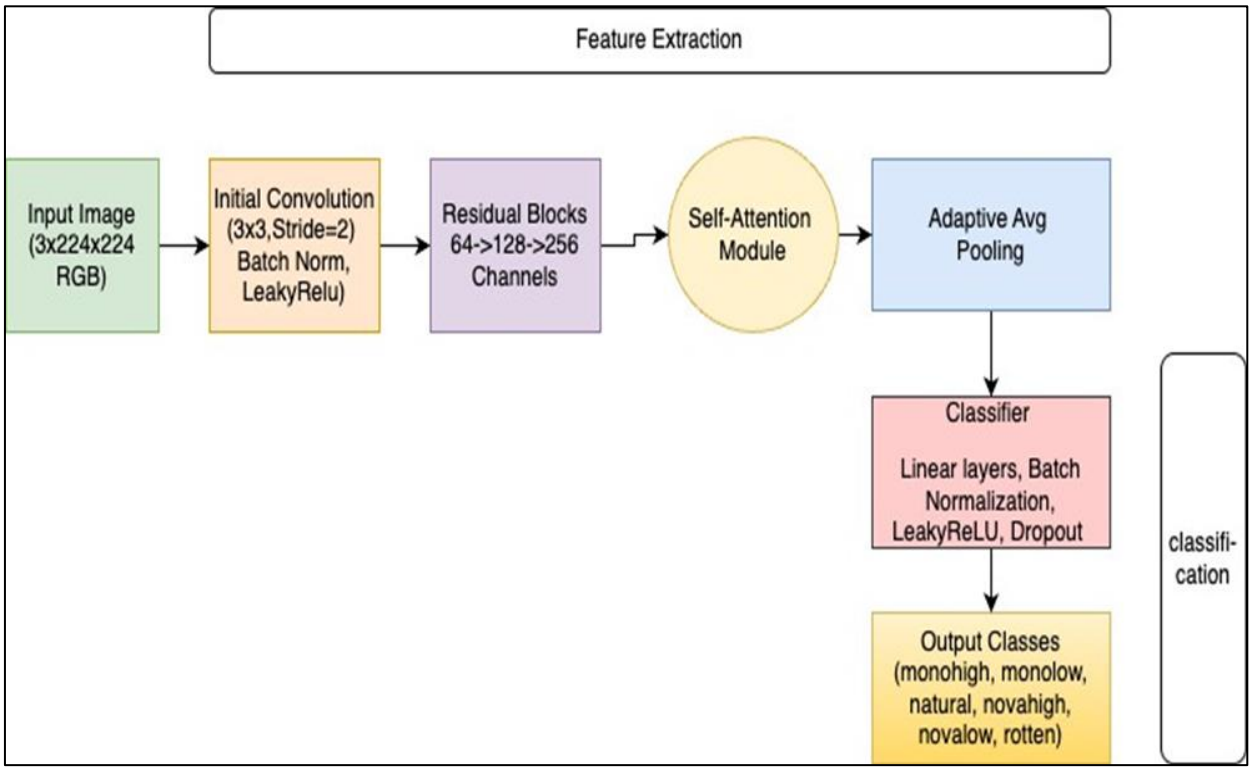

Figure 6. Proposed Methodology of Pesticide Classification

4.5 Model Training

The validate model command performs model testing by disabling gradient calculations and entering eval() mode (disabling dropout/batch normalization). It then traverses the validation batches, calculates prediction accuracy, and collects all the predictions/labels to measure performance. It transfers data to the target device (GPU/CPU), calculates model outputs, retrieves predicted classes using torch.max (argmax), and stores predictions/labels in the CPU to calculate the metrics for every batch. The purpose is to keep track of total samples and correct predictions to calculate accuracy, while also yielding a complete set of prediction-label pairs to enable detailed metrics such as confusion matrices or F1 scores. This architecture offers memory efficiency (in terms of batch processing) and reproducibility (detached tensors) that is suitable for testing chemical classification models, where performance or certainty of decision within each class is of interest. All the gathered predictions and labels can be utilized later in combination with other libraries like scikit-learn to perform additional analytics.

The train model line initiates the training process of the ChemNet model within a stipulated time frame in terms of epochs. The call to the function uses the train model function mentioned above, which takes essential inputs: the model architecture (model), training data loader (train loader), validation data loader (val loader), loss function (criterion), and optimizer. The model will repeatedly perform forward and backward passes on batches of training data to minimize the loss in each epoch. After the training for each epoch is complete, the model's performance will be tested using the validation data loader to determine its generalization capacity. This cyclical process allows for continual refinement of the accuracy and reliability of the model in predicting chemical classifications, and performance statistics are printed at the end of each epoch to monitor progress and guide any potentially necessary changes to the training strategy or hyperparameters. The confusion matrix measures the performance of a model on a validation dataset and displays the outputs in a confusion matrix. This function retrieves predictions and true labels of all examples using the validate model, then computes the confusion matrix and other important measures such as accuracy, precision, recall, and F1-score. It is important to note that these measures are scaled by a reference value, which seems to be in error (in most cases, metrics are scaled by 100 to represent a percentage). The seaborn heatmap is plotted with annotations and labeled axes to indicate the predicted and actual classes. Finally, the function prints the measures and shows the plot. This provides a full perspective of the classification performance of the model in terms of the strengths and weaknesses of the classes. The scaling factor ref should probably be set to 100 in order to achieve a normal percentage interpretation.

4.6 Model Parameters

Parameters of each layers are shown below

Layer	Output Shape	Parameters
Conv2d-1	[-1, 32, 112, 112]	896
BatchNorm2d-2	[-1, 32, 112, 112]	64
LeakyReLU-3	[-1, 32, 112, 112]	0
Conv2d-4	[-1, 64, 112, 112]	18,432
BatchNorm2d-5	[-1, 64, 112, 112]	128
LeakyReLU-6	[-1, 64, 112, 112]	0
Conv2d-7	[-1, 64, 112, 112]	36,864

BatchNorm2d-8	[-1, 64, 112, 112]	128
AdaptiveAvgPool2d-9	[-1, 64, 1, 1]	0
Linear-10	[-1, 4]	256
ReLU-11	[-1, 4]	0
Linear-12	[-1, 64]	256
Sigmoid-13	[-1, 64]	0
SEBlock-14	[-1, 64, 112, 112]	0
Conv2d-15	[-1, 64, 112, 112]	2048
BatchNorm2d-16	[-1, 64, 112, 112]	128
ResidualBlock-17	[-1, 64, 112, 112]	0
Conv2d-18	[-1, 64, 112, 112]	36,864
BatchNorm2d-19	[-1, 64, 112, 112]	128
LeakyReLU-20	[-1, 64, 112, 112]	0
Conv2d-21	[-1, 64, 112, 112]	36,864
BatchNorm2d-22	[-1, 64, 112, 112]	128
AdaptiveAvgPool2d-23	[-1, 64, 1, 1]	0
Linear-24	[-1, 4]	256
ReLU-25	[-1, 4]	0
Linear-26	[-1, 64]	256
Sigmoid-27	[-1, 64]	0
SEBlock-28	[-1, 64, 112, 112]	0
ResidualBlock-29	[-1, 64, 112, 112]	0
Conv2d-30	[-1, 128, 56, 56]	73,728
BatchNorm2d-31	[-1, 128, 56, 56]	256
LeakyReLU-32	[-1, 128, 56, 56]	0
Conv2d-33	[-1, 128, 56, 56]	147,456
BatchNorm2d-34	[-1, 128, 56, 56]	256
AdaptiveAvgPool2d-35	[-1, 128, 1, 1]	0
Linear-36	[-1, 8]	1024
ReLU-37	[-1, 8]	0
Linear-38	[-1, 128]	1024
Sigmoid-39	[-1, 128]	0
SEBlock-40	[-1, 128, 56, 56]	0
Conv2d-41	[-1, 128, 56, 56]	8192
BatchNorm2d-42	[-1, 128, 56, 56]	256
ResidualBlock-43	[-1, 128, 56, 56]	0
Conv2d-44	[-1, 128, 56, 56]	147,456
BatchNorm2d-45	[-1, 128, 56, 56]	256
LeakyReLU-46	[-1, 128, 56, 56]	0
Conv2d-47	[-1, 128, 56, 56]	147,456
BatchNorm2d-48	[-1, 128, 56, 56]	256
AdaptiveAvgPool2d-49	[-1, 128, 1, 1]	0
Linear-50	[-1, 8]	1024
ReLU-51	[-1, 8]	0
Linear-52	[-1, 128]	1024
Sigmoid-53	[-1, 128]	0
SEBlock-54	[-1, 128, 56, 56]	0
ResidualBlock-55	[-1, 128, 56, 56]	0
Conv2d-56	[-1, 256, 28, 28]	294,912

BatchNorm2d-57	[-1, 256, 28, 28]	512
LeakyReLU-58	[-1, 256, 28, 28]	0
Conv2d-59	[-1, 256, 28, 28]	589,824
BatchNorm2d-60	[-1, 256, 28, 28]	512
AdaptiveAvgPool2d-61	[-1, 256, 1, 1]	0
Linear-62	[-1, 16]	4096
ReLU-63	[-1, 16]	0
Linear-64	[-1, 256]	4096
Sigmoid-65	[-1, 256]	0
SEBlock-66	[-1, 256, 28, 28]	0
Conv2d-67	[-1, 256, 28, 28]	32,768
BatchNorm2d-68	[-1, 256, 28, 28]	512
ResidualBlock-69	[-1, 256, 28, 28]	0
Conv2d-70	[-1, 256, 28, 28]	589,824
BatchNorm2d-71	[-1, 256, 28, 28]	512
LeakyReLU-72	[-1, 256, 28, 28]	0
Conv2d-73	[-1, 256, 28, 28]	589,824
BatchNorm2d-74	[-1, 256, 28, 28]	512
AdaptiveAvgPool2d-75	[-1, 256, 1, 1]	0
Linear-76	[-1, 16]	4096
ReLU-77	[-1, 16]	0
Linear-78	[-1, 256]	4096
Sigmoid-79	[-1, 256]	0
SEBlock-80	[-1, 256, 28, 28]	0
ResidualBlock-81	[-1, 256, 28, 28]	0
Conv2d-82	[-1, 256, 28, 28]	589,824
BatchNorm2d-83	[-1, 256, 28, 28]	512
LeakyReLU-72	[-1, 256, 28, 28]	0
Conv2d-73	[-1, 256, 28, 28]	589,824
BatchNorm2d-74	[-1, 256, 28, 28]	512
AdaptiveAvgPool2d-75	[-1, 256, 1, 1]	0
Linear-76	[-1, 16]	4096
ReLU-77	[-1, 16]	0
Linear-78	[-1, 256]	4096
Sigmoid-79	[-1, 256]	0
SEBlock-80	[-1, 256, 28, 28]	0
ResidualBlock-81	[-1, 256, 28, 28]	0
Conv2d-82	[-1, 256, 28, 28]	589,824
BatchNorm2d-83	[-1, 256, 28, 28]	512
LeakyReLU-84	[-1, 256, 28, 28]	0
Conv2d-85	[-1, 256, 28, 28]	589,824
BatchNorm2d-86	[-1, 256, 28, 28]	512
AdaptiveAvgPool2d-87	[-1, 256, 1, 1]	0
Linear-88	[-1, 16]	4096
ReLU-89	[-1, 16]	0
Linear-90	[-1, 256]	4096
Sigmoid-91	[-1, 256]	0
SEBlock-92	[-1, 256, 28, 28]	0
ResidualBlock-93	[-1, 256, 28, 28]	0

Conv2d-94	[-1, 32, 28, 28]	8224
Conv2d-95	[-1, 32, 28, 28]	8224
Conv2d-96	[-1, 256, 28, 28]	65,792
SelfAttention-97	[-1, 256, 28, 28]	0
AdaptiveAvgPool2d-98	[-1, 256, 1, 1]	0
Flatten-99	[-1, 256]	0
Linear-100	[-1, 512]	131,584
BatchNorm1d-101	[-1, 512]	1024
LeakyReLU-102	[-1, 512]	0
Dropout-103	[-1, 512]	0
Linear-104	[-1, 256]	131,328
BatchNorm1d-105	[-1, 256]	512
LeakyReLU-106	[-1, 256]	0
Dropout-107	[-1, 256]	0
Linear-108	[-1, 10]	2570

Total params	4,317,578
Trainable params	4,317,578
Non-trainable params	0
Input size (MB)	0.57
Forward/backward pass size (MB)	194.91
Params size (MB)	16.47
Estimated Total Size (MB)	211.95

4.7 Implementation Details

The neural network model (ChemNet) is ready to be trained, or inference is run. First, it verifies that a GPU is available with PyTorch and, if possible, sets the computation device to CUDA (GPU) otherwise, it uses the CPU. It is then instantiated as a model (num classes=e.g., 10 classes in the case of classification, input channels=3 in the case of RGB images) and transferred to the chosen device via .to(device) in order to use GPU acceleration. Its input size is (3, 224, 224) which is the standard size of the input (channels, height, width) of a model such as ResNet. Lastly, the summary operation (probably torchinfo or torchsummary) produces a complete summary of the model architecture and shows the layer-by-layer statistics, output dimensions, and memory requirements to check the network structure as well as to ensure that it will work with the size of the input. This arrangement is to ensure that the model is correctly set up to be effectively trained or evaluated on accessible hardware.

The given model summary shows that there are 4,317,578 parameters in the neural network, all of which are trainable parameters, i.e., they are to be updated during the training process. All parameters are trainable, and they do not include the frozen weights or those that are not updated during training. The input size is approximately 0.57 MB but the memory required for a forward and backward pass is significantly larger with the values reaching 194.91 MB. The parameters of the model by themselves occupy approximately 16.47 MB of memory. The approximate size of the estimated model, including input, forward/backward passes, and parameters is approximately 211.95 MB. Such a summation provides immense insights into

the complexity of the model and memory consumption, which are vital in optimizing resource usage and performance during training and deployment.

4.8 Evaluation Criteria

The evaluation criteria are relevant ways to scrutinize the competency and effectiveness of a method. Based on this, the evaluation metrics proposed to approximate the recommended architecture are Accuracy, Precision, Recall and F1 Score. These are explained as follows: Table 4 presents the most important evaluation metrics applied to evaluate the performance of the proposed model of insecticide classification, such as accuracy, precision, recall, and F1-score. These parameters are important in the interpretation of the model with respect to its capability of recognizing and categorizing various bug-killers.

Accuracy denotes the percentage of correct predictions of the model across all classes. It is obtained by the formula:

$$Accuracy = \frac{TP + TN}{TP + TN + FP + FN}$$

TP: True Positives

TN: True Negatives

FP: False Positives

FN: False Negatives

The accuracy of the proposed model was 81.02%, which means that the number of correct predictions was about 8 correct predictions out of 10, demonstrating the overall effectiveness of the model in dealing with the classification problem.

Precision is used to measure the rate of true positive predictions to the total positive predictions the model makes. It is a measure of how well the model avoids false positives.

It is a formula where:

$$Precision = \frac{TP}{TP + FP}$$

The model has a strong sense of reliability in its positive predictions;85.34% of the cases of insecticide are identified correctly with minimal false positives.

Recall measures the capacity of the model to recognize all the relevant cases (i.e. all true positives). It has special importance when the cost of failing to detect a positive case is high.

The formula is:

$$Recall = \frac{TP}{TP + FN}$$

An 81.02% recall means that the model has managed to recall a substantial proportion of the actual insecticide cases, which is important in the actual detection application, where omitting contaminants may present dangerous health implications.

The F1-score is the harmonic average of precision and recall providing a balanced measure, which takes false negatives and false positives into account. It is calculated as:

$$F1\ Score = 2 * \frac{Precision * Recall}{Precision\ +\ Recall}$$

The training epochs, learning rate, and batch size are hyperparameters. This has been done repeatedly in such a way that the best training environment, which would not only maximize the accuracy of the model but also provide stable and convergent training, would be achieved. The learning rate was the determinant of the balance between training pace and training steadiness, and the training behavior was influenced by the batch size, although both had an impact on the generation capability.

The test set classification accuracy of the modified ChemNet topped 81% after the final evaluation, not bad given that the insecticides were highly heterogeneous in structure. The model framework was developed as a tool to accommodate the domain-specific information of the chemistry that enabled the isolation of the multifaceted relationships in the properties of the molecule and to come up with the most definitive classes.

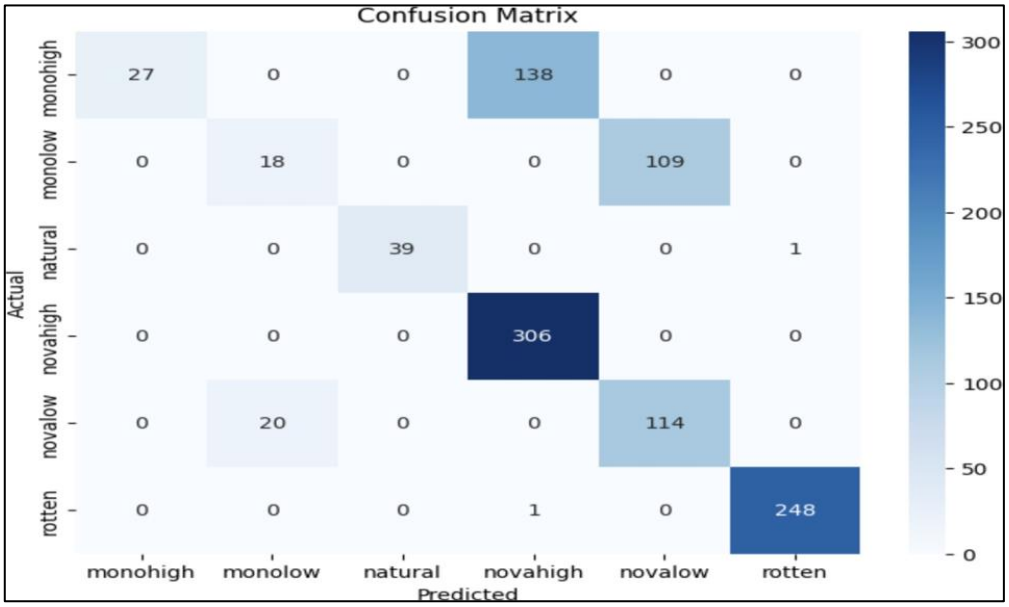

Figure 7. Confusion Matrix

As shown in Figure 7, the confusion matrix evidences that the suggested Modified ChemNet model shows a high level of classification performance in all six insecticide exposure categories. Monohigh and novahigh are highly accurate, and there are few misclassifications in the case of novalow and natural, which means that these two groups are similar visually. This demonstrates the ability of SE blocks and the attention module to improve feature discrimination. A confusion matrix is a summary of the model's performance regarding the numbers of TP, TN, FP, and FN predictions. The computation of important performance measures such as precision, recall, and F1 also depends on the matrix, accuracy score, and overall accuracy. The training confusion matrix assesses the model's performance using the

training dataset and detects overfitting or underfitting problems. Figure 8 depicts the confusion matrix that gives a graphical representation of the model's predictions within the banana insecticide datasets. Confusion matrix analysis further shows the performance of the model on an individual class. The findings revealed that Modified ChemNet was consistent in most categories of insecticides. However, there was a slight reduction in accuracy for the classes containing rare chemical scaffolds, which were poorly represented in the training set. This highlights a general issue in cheminformatics: learning biased or uncommon molecular patterns. The accuracy of the model and the training loss are plotted in Figure 8.

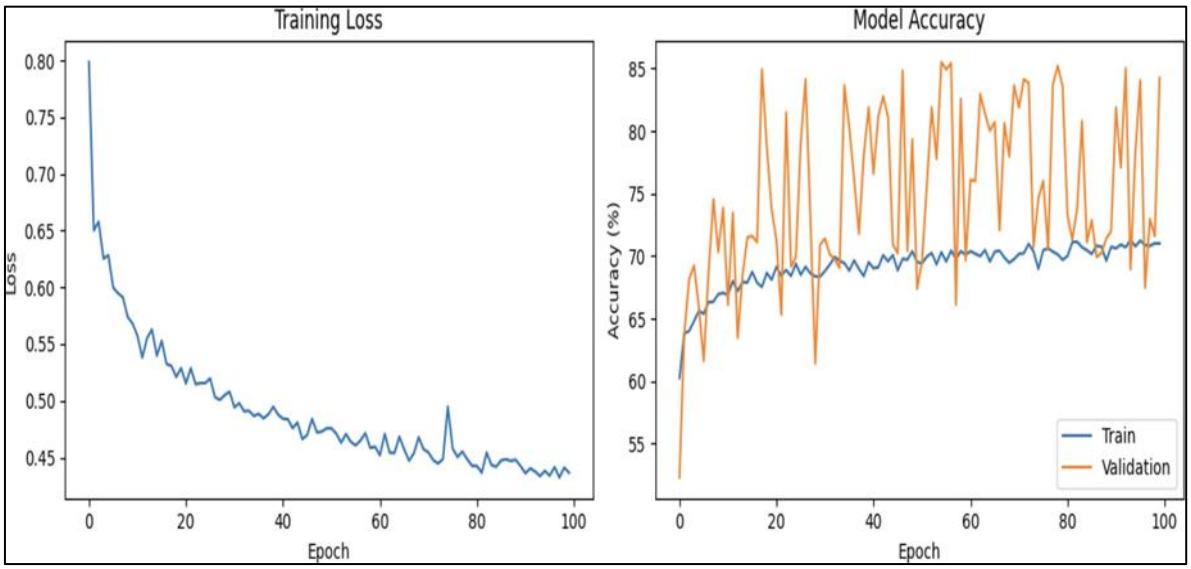

Figure 8. Accuracy and Loss Graph

Figure 8 shows that training accuracy increases steadily and approaches an accuracy of approximately 81.01%. This indicates a good generalization of the model without significant overfitting. This confirms the effects of the Swish activation function and cyclic learning rate scheduling. Figure 8 also shows trends in training loss. Loss decreases slowly and reaches epoch 40, demonstrating stable optimization. This monotonic decline highlights the benefits of both early stopping and class balancing in preventing overfitting and underfitting.

However, the general results of the studies are more favorable toward the utility of ChemNet and other chemically informed neural networks in the automatic classification of compounds, due to their generalizability, even among structurally diverse insecticides, and their applicability in the real world for pesticide recognition, regulatory screening, and environmental safety.

Table 4. Proposed Model Results

Model	Accuracy	Precision	Recall	F1 Score
Proposed Model	81.01%	85.33%	81.01%	75.04%

Table 4 shows the results of the proposed model. The specified model recorded an accuracy of 81.02%, a precision of 85.34%, a recall of 81.02% and an F1 score of 75.04%. Figure 9. presents the performance metrics for the testing data,

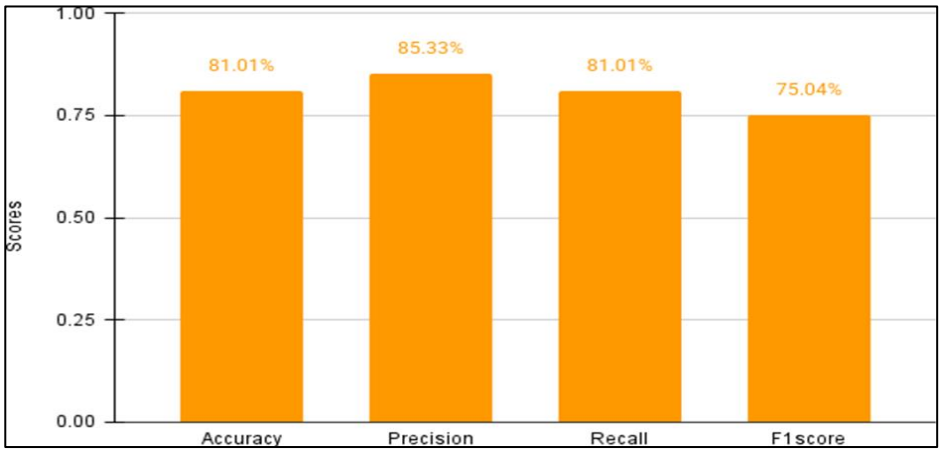

Figure 9. Performance Metrics for Testing Data

4.9 Comparison with traditional models

Table 5 provides a comparative overview of some traditional deep learning approaches employed in fruit classification and pesticide detection problems, along with the development of model performance in various research works. In most past models, relatively simple CNN structures, such as 3-layer networks or versions of LeNet, have been applied to fruits like mangoes, apples, tomatoes, and grapes. The accuracy of these models was usually mediocre (75.6-80.1%), and they tended to perform poorly due to limitations such as small data sets, lack of data augmentation, shallow feature extraction, and poor adaptation to spectral variability. For example, Jiang et al.[32] applied the SVM model and achieved an accuracy of 73.20%, which is confined to one experimental dataset. Differences in lighting, temperature, and leaf texture were not taken into account. Analysis by Alghawas et al.[34] showed that the machine learning models used in their study attained an overall accuracy of 75% in detecting pesticide residues. Figure 10 indicates the comparison of accuracy among deep learning models in detecting pesticides, demonstrating that these models have high potential for detecting residues in food samples. Overall, the limitations of the paper raise the following issues: the representativeness of data, the variability of model performances, the problem of an unbalanced data set, the possibility of missing variables, and the necessity for more sophisticated modeling methods. These factors should be considered when interpreting the results and transferring them to general contexts. The new ChemNet model, specifically trained with a chemically aware architecture, outperformed these previous models with an accuracy of 81.01% on banana samples. The model demonstrated superior generalization, especially across insecticide classes of different chemical structures, validating its usefulness in the automated detection of pesticides in crops.

Table 5. Comparison of Traditional Model Accuracy with Proposed Model

Author(s)	Model/ Approach	Accuracy	Notes
Jiang et.al. [32]	SVM	73.20%	Currently limited to a single experimental dataset

			Variations in lighting, temperature, and leaf texture were not considered
Alghawas et al. [34]	KNN, Logistic Regression, Na¨ıve Bayes, S V M	75%	Real-world dataset; identifies improvement areas and contributes to better food safety practices
Proposed Model	ChemNet Architecture	81.01%	Shows effective generalization across structurally diverse insecticide classes.

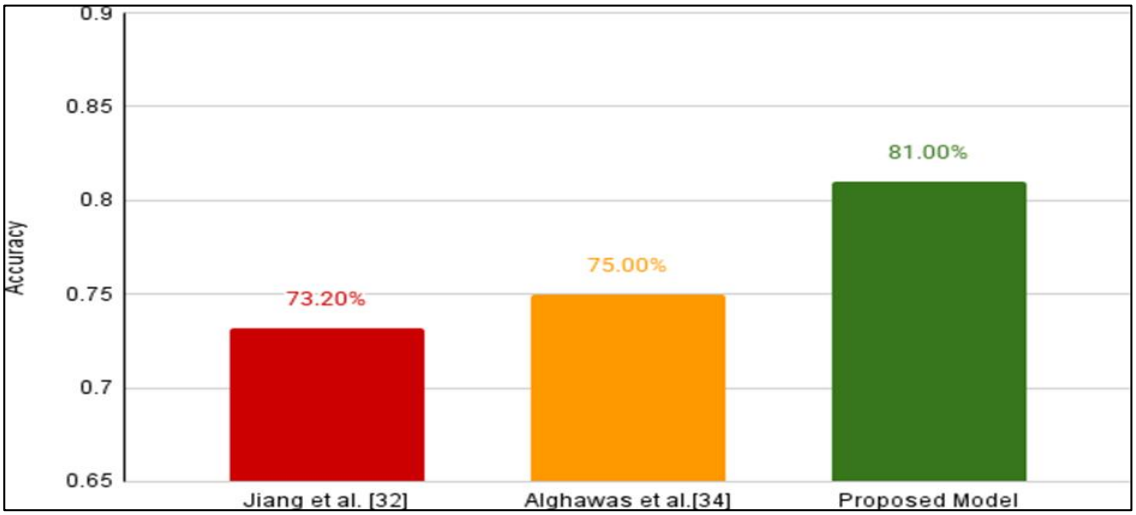

Figure 10. Comparison of Accuracy of Deep Learning Models for Pesticide Detection

5. Conclusion

This paper presents a slight modification to the ChemNet architecture to detect insecticide residues on fruits specifically bananas. The incorporation of the latest components like Squeeze-and-Excitation (SE) blocks, Residual Units, and Self-Attention mechanism allowed the model to extract the chemically important features and spatial patterns related to the presence of pesticides contamination. The proposed model was tested on a heterogeneous and diverse banana insecticide dataset. The model produced a classification accuracy rate of 81.02%, a precision rate of 85.34%, a recall rate of 81.02%, and an F1-score of 75.04%. These findings indicate that the enhanced ChemNet is considerably more precise and general than the conventional models (SVM and simple CNNs) especially when applied to insecticides that are structurally different.

Moreover, the fact that this model can perform consistently across different classes, even when the patterns representing them are visually similar, or rare, demonstrates its strength and applicability in real-world settings. The confusion and comparative evaluation demonstrate the high generalization ability of the proposed system. This study forms the basis for implementing automated pesticide detection systems using deep learning for agricultural inspections and food safety monitoring. In the future, it will be investigated how to incorporate multi-modal data fusion, spectral-spatial attention, and ensemble learning to make the models more accurate and reliable.

References

[1] Philippe, Verger, Agamy Neveen, Anshasi Marwa, and Al-Yousfi Ahmad Basel. "Occurrence of pesticide residues in fruits and vegetables for the Eastern Mediterranean Region and potential impact on public health." Food Control 119 (2021): 107457.

[2] Kazimierczak, Renata, Dominika Średnicka-Tober, Jan Golba, Anna Nowacka, Agnieszka Hołodyńska-Kulas, Klaudia Kopczyńska, Rita Góralska-Walczak, and Bogusław Gnusowski. "Evaluation of pesticide residues occurrence in random samples of organic fruits and vegetables marketed in Poland." Foods 11, no. 13 (2022): 1963.

[3] Granados-Povedano, Mireya, Irene Domínguez, Francisco Egea-González, Antonia Garrido Frenich, and Francisco Javier Arrebola. "Unified method for target and non-target monitoring of pesticide residues in fruits and fruit juices by gas chromatography-high resolution mass spectrometry." Foods 12, no. 4 (2023): 739.

[4] El-Sheikh, El-Sayed A., Mahmoud M. Ramadan, Ahmed E. El-Sobki, Ali A. Shalaby, Mark R. McCoy, Ibrahim A. Hamed, Mohamed-Bassem Ashour, and Bruce D. Hammock. "Pesticide residues in vegetables and fruits from farmer markets and associated dietary risks." Molecules 27, no. 22 (2022): 8072.

[5] Evarist, Nabaasa, Natumanya Deborah, Grace Birungi, Nakiguli Kiwanuka Caroline, and Baguma John Muhunga Kule. "A model for detecting the presence of pesticide residues in edible parts of tomatoes, cabbages, carrots, and green pepper vegetables." In Artificial Intelligence and Applications, vol. 2, no. 3, (2024): 196-203.

[6] Hu, Yating, Benxue Ma, Huting Wang, Yuanjia Zhang, Yujie Li, and Guowei Yu. "Detecting different pesticide residues on Hami melon surface using hyperspectral imaging combined with 1D-CNN and information fusion." Frontiers in Plant Science 14 (2023): 1105601.

[7] Borza, Gavrilă, Luana PĂCURAR, Florin Russu, Ioan Gaga, Sebastian CHIRIŢĂ, Teodora Florian, Ioan Oltean, Raluca Rezi, and Camelia Urdă. "Influence of insecticides for stored grain protection on the technological properties of winter wheat." AgroLife Scientific Journal 11, no. 2 (2022).

[8] Kang, Zhilong, Yuchen Zhao, Lei Chen, Yanju Guo, Qingshuang Mu, and Shenyi Wang. "Advances in machine learning and hyperspectral imaging in the food supply chain." Food Engineering Reviews 14, no. 4 (2022): 596-616.

[9] Li, Min, Linju Lu, and Xiaoying Zhang. "Qualitative determination of pesticide residues in purple cabbage based on near infrared spectroscopy." In Journal of Physics: Conference Series, vol. 1884, no. 1, p. 012015. IOP Publishing, 2021.

[10] Gowen, Aoife A., Colm P. O'Donnell, Patrick J. Cullen, Gérard Downey, and Jesus M. Frias. "Hyperspectral imaging–an emerging process analytical tool for food quality and safety control." Trends in food science & technology 18, no. 12 (2007): 590-598.

[11] Moeder, M., C. Bauer, P. Popp, M. Van Pinxteren, and T. Reemtsma. "Determination of pesticide residues in wine by membrane-assisted solvent extraction and high-performance liquid chromatography–tandem mass spectrometry." Analytical and bioanalytical chemistry 403, no. 6 (2012): 1731-1741.

[12] Bouagga, A., H. Chaabane, Khaoula Toumi, A. Mougou Hamdane, B. Nasraoui, and Laure Joly. "Pesticide residues in Tunisian table grapes and associated risk for consumer's health." Food Additives & Contaminants: Part B 12, no. 2 (2019): 135-144.

[13] Narenderan, S. T., S. N. Meyyanathan, and B. J. F. R. I. Babu. "Review of pesticide residue analysis in fruits and vegetables. Pre-treatment, extraction and detection techniques." Food Research International 133 (2020): 109141.

[14] Simonetti, Giulia, Federica Castellani, Patrizia Di Filippo, Carmela Riccardi, Donatella Pomata, Roberta Risoluti, Francesca Buiarelli, and Elisa Sonego. "Determination of Mancozeb, a pesticide used worldwide in agriculture: comparison among GC, LC, and CE." Current Analytical Chemistry 16, no. 8 (2020): 1041-1053.

[15] Grimalt, Susana, and Pieter Dehouck. "Review of analytical methods for the determination of pesticide residues in grapes." Journal of Chromatography A 1433 (2016): 1-23.

[16] Pérez-Navarro, José, Pedro Miguel Izquierdo-Cañas, Adela Mena-Morales, Jesús Martínez-Gascueña, Juan Luis Chacón-Vozmediano, Esteban García-Romero, Isidro Hermosín-Gutiérrez, and Sergio Gómez-Alonso. "Phenolic compounds profile of different berry parts from novel Vitis vinifera L. red grape genotypes and Tempranillo using HPLC-DAD-ESI-MS/MS: A varietal differentiation tool." Food chemistry 295 (2019): 350-360.

[17] Zhang, Xinzhong, Yuechen Zhao, Xinyi Cui, Xinru Wang, Huishan Shen, Zongmao Chen, Chun Huang et al. "Application and enantiomeric residue determination of diniconazole in tea and grape and apple by supercritical fluid chromatography coupled with quadrupole-time-of-flight mass spectrometry." Journal of Chromatography a 1581 (2018): 144-155.

[18] Baca-Bocanegra, Berta, José Miguel Hernández-Hierro, Julio Nogales-Bueno, and Francisco José Heredia. "Feasibility study on the use of a portable micro near infrared spectroscopy device for the "in vineyard" screening of extractable polyphenols in red grape skins." Talanta 192 (2019): 353-359.

[19] Lemos, André Mendes, Nelson Machado, Marcos Egea-Cortines, and Ana Isabel Barros. "ATR-MIR spectroscopy as a tool to assist 'Tempranillo'clonal selection process: Geographical origin and year of harvest discrimination and oenological parameters prediction." Food Chemistry 325 (2020): 126938.

[20] Fernández-Novales, Juan, Javier Tardáguila, Salvador Gutiérrez, and María Paz Diago. "On-The-Go VIS+ SW− NIR spectroscopy as a reliable monitoring tool for grape composition within the vineyard." Molecules 24, no. 15 (2019): 2795.

[21] dos Santos Costa, Daniel, Nelson Felipe Oliveros Mesa, Murilo Santos Freire, Rodrigo Pereira Ramos, and Barbara Janet Teruel Mederos. "Development of predictive models for quality and maturation stage attributes of wine grapes using vis-nir reflectance spectroscopy." Postharvest Biology and Technology 150 (2019): 166-178.

[22] Sun, Jun, Sunli Cong, Hanping Mao, Xiaohong Wu, and Ning Yang. "Quantitative detection of mixed pesticide residue of lettuce leaves based on hyperspectral technique." Journal of Food Process Engineering 41, no. 2 (2018): e12654.

[23] Jia, Yaguang, Jinrong He, Hongfei Fu, Xiatian Shao, and Zhaokui Li. "Apple surface pesticide residue detection method based on hyperspectral imaging." In International Conference on Intelligent Science and Big Data Engineering, Cham: Springer International Publishing, (2018): 539-556.

[24] Hussain, Saqib, Tariq Masud, and Karam Ahad. "Determination of pesticides residues in selected varieties of mango." Pakistan Journal of Nutrition 1, no. 1 (2002): 41-42.

[25] Sultana, Farhana, Abu Sufian, and Paramartha Dutta. "Advancements in image classification using convolutional neural network." In 2018 Fourth international conference on research in computational intelligence and communication networks (ICRCICN), IEEE, (2018): 122-129.

[26] TAHIR ANWAR, IMTIAZ AHMAD, and SEEMA TAHIR. "Determination of pesticide residues in fruits of Nawabshah district, Sindh, Pakistan." Pak. J. Bot 43, no. 2 (2011): 1133-1139.

[27] Omoyajowo, Koleayo, K. Njok, Sunday Amiolemen, John Ogidan, Olapeju Adenekan, Kayode Olaniyan, Julie Akande, and Ifeoluwa Idowu. "Assessment of pesticide residue levels in common fruits consumed in Lagos State, Nigeria." Journal of Research and Reviews in Science. https: Sciencejournal. lasucomputerscience. co m (2018): 56-62.

[28] Srivastava, Ashutosh K., Satyajeet Rai, M. K. Srivastava, M. Lohani, M. K. R. Mudiam, and L. P. Srivastava. "Determination of 17 organophosphate pesticide residues in mango by modified QuEChERS extraction method using GC-NPD/GC-MS and hazard index estimation in Lucknow, India." PloS one 9, no. 5 (2014): e96493.

[29] Mammoo, Jubaira, P. Malin Bruntha, and Avik Saha. "Detecting Pesticide Contamination in Fruits and Vegetables with Deep Learning Models." In 2025 6th International Conference on Mobile Computing and Sustainable Informatics (ICMCSI), IEEE, (2025): 1084-1090.

[30] Jiang, Rongchang, Guoqiang Zhuang, Shijie Xie, Yang Wang, Guoqi Zhang, Dandan Qu, and Wanzhi Wen. "Hyperspectral Detection of Pesticide Residues in Black Vegetable Based on Multi-classifier Entropy Weight Method." IEEE Access (2025).

[31] Mammoo, Jubaira, and P. Malin Bruntha. "Efficient Siamese Pyramid Attention Network with Fusion Autoencoder and Hypercube Gan for Detection of Pesticide Residue." Journal of Circuits, Systems and Computers 34, no. 11 (2025): 2550266.

[32] Alghawas, Masooma, and Sawsan Hilal. "Comparison Analysis of Machine Learning Models for Identification of Pesticide Residue." In 2024 5th International Conference on Data Analytics for Business and Industry (ICDABI), IEEE, (2024): 128-131